



# Study of the consumption of the additive prop-1-ene-1,3-sultone in Li [Ni<sub>0.33</sub>Mn<sub>0.33</sub>Co<sub>0.33</sub>]O<sub>2</sub>/graphite pouch cells and evidence of positive-negative electrode interaction

R. Petibon <sup>a</sup>, L. Madec <sup>b</sup>, L.M. Rotermund <sup>b</sup>, J.R. Dahn <sup>a, b, \*</sup>

<sup>a</sup> Dept. of Chemistry, Dalhousie University, Halifax, Nova Scotia, B3H 4R2, Canada

<sup>b</sup> Dept. of Physics and Atmospheric Science, Dalhousie University, Halifax, Nova Scotia, B3H 4R2, Canada

## HIGHLIGHTS

- The consumption of the additive prop-1-ene-1,3-sultone (PES) was studied.
- Li[Ni<sub>0.33</sub>Mn<sub>0.33</sub>Co<sub>0.33</sub>]O<sub>2</sub>/graphite pouch cells cycled to 4.2 V were used.
- PES is partially consumed at the positive electrode at 4.2 V.
- A positive-negative electrode interaction exists in full cells operated to 4.2 V.
- The negative electrode impedance was greatly affected by this interaction.

## ARTICLE INFO

### Article history:

Received 10 September 2015

Received in revised form

14 January 2016

Accepted 16 February 2016

Available online 19 March 2016

### Keywords:

Lithium-ion batteries

Additive

Prop-1-ene-1,3-sultone

Consumption

Interaction

Li[Ni<sub>x</sub>Mn<sub>y</sub>Co<sub>1-x-y</sub>]O<sub>2</sub>/graphite cells

## ABSTRACT

The consumption of the additive prop-1-ene-1,3-sultone (PES) in Li[Ni<sub>0.33</sub>Mn<sub>0.33</sub>Co<sub>0.33</sub>]O<sub>2</sub>/graphite (NMC(111)/graphite) pouch cells during the first cycle and after hold periods at different cell potentials was measured using gas chromatography coupled with mass spectrometry (GC-MS). GC-MS measurements of the electrolyte of NMC(111)/graphite pouch cells during the first charge showed that the amount of PES consumed, and the cell impedance, increased with increasing starting concentration up to a starting concentration of 5 wt% and then seemed to slow down at higher starting concentration. Additive consumption measurements after holding periods showed that PES is consumed in measurable amounts at the positive electrode, suggesting that PES oxidizes at potentials as low as 4.27 V vs. Li/Li<sup>+</sup> on the NMC(111) surface. Electrochemical impedance spectroscopy on symmetric cells as well as X-ray photoelectron spectroscopy of electrodes salvaged from NMC(111)/graphite cells after hold periods at various cell potentials strongly support the existence of a positive-negative electrode interaction.

© 2016 Elsevier B.V. All rights reserved.

## 1. Introduction

Li-ion battery-powered vehicles and grid storage units are a commercial reality, but cost is still too steep. In order to make them less expensive, the cost per kWh as well as the cost per cycle should be minimized. While the cost per kWh depends greatly on raw material cost, the cost per cycle strongly depends on cell lifetime.

Electrolyte additives have been widely used in order to tune lifetime [1–3], with vinylene carbonate (VC) being the most studied

[1,4–8]. Recently, Li et al. reported that prop-1-ene-1,3-sultone (PES) allows propylene carbonate to be used with graphitic negative electrodes without the need for other passivating compounds such as ethylene carbonate (EC) or VC [9,10]. Surface analysis [10] suggested that PES is reduced at the graphite electrode where it forms a passivating film. Later Xia et al. showed that PES provided high coulombic efficiency, low parasitic oxidation currents and low gas production when added to an EC-based electrolyte of NMC(111)/graphite pouch cells cycled up to 4.2 V at both 40 °C and 60 °C [11]. Madec et al. [12] recently published a X-ray photoelectron spectroscopy (XPS) study of the surface of the electrodes of NMC(111)/graphite cells filled with EC-based electrolyte containing PES. In their publication, Madec et al. showed that PES strongly affected the composition of the solid electrolyte interphase (SEI) of

\* Corresponding author. Dept. of Physics and Atmospheric Science, Dalhousie University, Halifax, Nova Scotia, B3H 4R2, Canada.

E-mail address: [jeff.dahn@dal.ca](mailto:jeff.dahn@dal.ca) (J.R. Dahn).

both the negative and positive electrodes. Generally, they found that the SEI at the positive electrode was thicker when PES was used. They also found that the SEI at both the positive and negative electrodes were more stable and contained sulfur-containing species.

Xia et al. [11] and Nelson et al. [13] showed that PES was as effective as an additive as VC with the added benefit of very low gas generation. In a later publication, Aiken et al. showed that the use of PES greatly helped minimize the volume of gas generated during the formation cycle of Li[Ni<sub>0.4</sub>Mn<sub>0.4</sub>Co<sub>0.2</sub>]O<sub>2</sub>/graphite pouch cells charged to high voltage (>4.5 V) [14]. Ma et al. [15] and Nelson et al. [16] showed that the use of ternary additive blends that include PES improved the performance of Li[Ni<sub>0.4</sub>Mn<sub>0.4</sub>Co<sub>0.2</sub>]O<sub>2</sub>/graphite cycled to high potential (4.4 V and above) compared to conventional additive blends containing VC.

While electrolyte additives are widely used, little about their mechanism of action is understood. For instance, until recently the extent of the consumption of an additive upon cell formation and subsequent cycling had never been reported in the open literature. Recently, Petibon et al. reported on an electrolyte extraction technique which allowed the concentration–time profile of additives to be followed by gas chromatography [17]. Using this technique, they studied the extent of the consumption of VC in NMC(111)/graphite cells during the first cycle and after different potential–hold periods [7]. They showed that VC was reduced throughout the first charge (formation cycle) of the cell and not just at the peak in dQ/dV vs. V. They also showed that the VC remaining after the first cycle was mainly consumed at the negative electrode during subsequent cell use. Lastly, they showed that the magnitude of the impedance of cells containing VC was roughly proportional to the amount of VC consumed regardless of the starting concentration. These measurements helped understand the reactivity of VC in the early life of a cell as well as during cell use.

Since PES has been shown to be a very promising additive, further studies focusing on its reactivity should be undertaken. In this article, the concentration profile of PES during the first charge of NMC(111)/graphite cells is measured. The effect of potential–holds at different cell potentials on the consumption of PES is reported. The individual electrode impedances and their surface chemistries were also evaluated. A variety of techniques such as GC–MS, electrochemical impedance spectroscopy on symmetric cells as well as XPS were used.

## 2. Experimental

### 2.1. Pouch cells and cell formation

Dry (no electrolyte) 220 mAh NMC(111)/graphite pouch cells were obtained from Li-Fun Technology (Xinma Industry Zone, Golden Dragon Road, Tianyuan District, Zhuzhou City, Hunan Province, PRC, 412000). The negative to positive active mass ratio of the NMC(111)/graphite cells was adjusted so the cells could be cycled to 4.2 V without lithium plating. The negative electrode consisted of 15–30 μm artificial graphite flakes blended with carbon black as conductive agent and carboxymethyl cellulose–styrene–butadiene rubber as binding agent, in a 96:2:2 wt ratio. The positive electrode consisted of 7–15 μm NMC(111) particles mixed with carbon black as conductive agent and polyvinylidene fluoride as binding agent in a weight ratio of 96:2:2. The specific procedures for electrolyte filling, cell sealing and cell formation can be found in an earlier publication [18].

### 2.2. Chemicals

The chemicals used in the electrolytes were obtained from BASF

(LiPF<sub>6</sub>, purity 99.94%, water content 14 ppm, EC:ethyl methyl carbonate (EMC), 3:7 by weight, water content < 20 ppm), and Lian-chuang Medicinal Chemistry Co., Ltd., China (Prop-1-ene-1,3-sultone (PES), purity 98.20%). The base electrolyte formulation, to which PES was added in this study, consisted of 1 M LiPF<sub>6</sub> EC:EMC (3:7 w:w) and is referred to as “control”. All additive concentrations reported in this article are relative to the total weight of the solvents and additives (the weight of the salt was not taken into account).

### 2.3. Electrochemical impedance spectroscopy

The electrochemical impedance spectra shown in this report were measured using a BioLogic VMP3 equipped with 2 EIS boards. All impedance measurements were made using a 20 mV input signal from 100 kHz to 100 mHz. The experimental setup did not allow for reproducible solution resistance measurements due to cable and connector impedance. For this reason, all impedance spectra were shifted so they would start at 5 Ω·cm<sup>2</sup> on the real axis at the highest frequency measured (x-axis intercept shifted to 5 Ω·cm<sup>2</sup>).

### 2.4. GC–MS measurements of the electrolyte

The measurement of the concentration of additive left in the cell after cycling was performed using the method described by Petibon et al. [17]. In this procedure, dichloromethane was used to extract the electrolyte from the jelly roll of the cell. The extracted electrolyte was then added to a mixture of dichloromethane and distilled water in a dichloromethane:water ratio of 100:1 (w:w). This step allowed potentially damaging chemicals such as PF<sub>5</sub> and HF to be removed. The organic phase was then injected in the GC–MS for the solvent and additive components of the electrolyte to be analyzed. The removal of corrosive chemicals prior to GC–MS injection protected the sensitive instrument components and yielded chromatograms free of silicate peaks due to column degradation. A detailed description of this method can be found in various publications [7,17–20].

Each data point presented in this article is the average of two measurements made on electrolyte extracted from two nominally identical cells (total of four measurements). The error bars of each data point are the standard deviation of these four measurements.

### 2.5. Symmetric cells constructed from pouch cells

The positive electrode and negative electrode symmetric cell construction using electrodes recovered from pouch cells followed the procedure described by Petibon et al. [21]. A detailed description of the procedure can be found in various publications [18,21–23]. Prior to symmetric cell assembly, pouch cells were charged to 3.80 V and held at that potential until the current dropped below C/1000.

### 2.6. X-ray photoelectron spectroscopy (XPS)

XPS was performed using a SPECS spectrometer equipped with a Phoibos 150 hemispherical energy analyzer and using Mg Kα radiation (hν = 1253.6 eV). The samples were transported from the Ar-filled glovebox to the XPS vacuum chamber without being exposed to the air. The sample preparation, sample transfer, XPS analysis and spectra fitting procedures can be found in Ref. [19].

In order to avoid presenting many XPS spectra and corresponding lengthy description, a Figure summarizing the XPS spectra is shown in this article. The detailed XPS core spectra, fitting of the peaks along with analysis of the spectra are presented in the

**supplementary information.** For the schematic representations of the SEI films, the SEI thicknesses were estimated using the relative intensity of the NMC active material feature, *i.e.* the NMC O<sup>1s</sup> feature at 529.5 eV. For the graphite electrode, SEI thicknesses were estimated using the graphite feature at about 282.5 eV.

The relative intensity was defined as:

$$I_{\text{rel}} = \text{at. \% (sample)} / \text{at. \% (fresh)} \quad (1)$$

Where at. % (sample) and at. % (fresh) are the atomic percentages of the active material feature of a given sample and for the fresh electrode, respectively, as determined from XPS quantification. Assuming a simple model where the SEI layer was considered as homogenous in thickness ( $d$ ) and with an average composition, the SEI thickness was then calculated as:

$$I_{\text{rel}} = e^{-d/\lambda} \quad (2)$$

where the inelastic mean free path (IMFP),  $\lambda$ , was calculated by averaging values for polyacetylene, LiF and polyethylene [24]. This procedure yields  $\lambda = 2.7$  nm and 2.1 nm for the photoelectron kinetic energies of  $\sim 1000$  eV (C 1s) and  $\sim 700$  eV (O 1s) used in this study.

### 3. Results and discussion

#### 3.1. Consumption during the first cycle

Fig. 1 shows the differential capacity vs. cell potential plot of the first charge of 220 mAh NMC(111)/graphite pouch cells filled with electrolytes containing either 2.2% VC (blue) or 2.2% PES (red). The amount of additive remaining in the cell is also shown (right y-axis) for selected cell potentials. The data for cells containing 2.2% VC were presented in an earlier publication [7]. The differential capacity plot of the first charge of cells containing VC shows a peak around 2.8 V while  $dQ/dV$  vs.  $V$  for cells containing PES shows a peak around 2.4 V. These two peaks correspond to the reduction of VC [1,25,26] and PES [9,11] at the graphite surface, respectively. The additive concentration data point at 0 V corresponds to cells that have been filled but not charged. This data point was measured in order to confirm the effectiveness of the extraction method. If the extraction method was incomplete, or the additive reacted during the extraction step involving the addition of water, the additive concentration measured would differ significantly from the

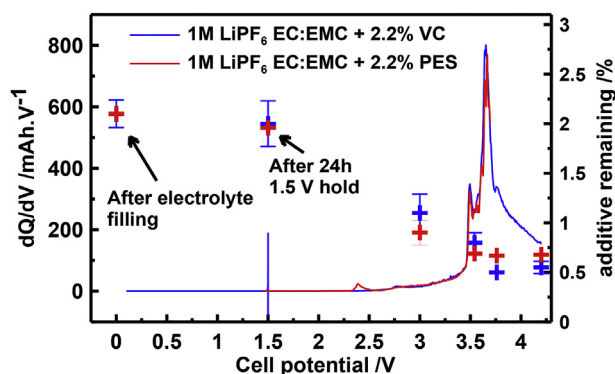


**Fig. 1.** Differential capacity vs. voltage of the first charge of NMC(111)/graphite pouch cells (left y-axis) initially containing 2.2% VC (blue) and 2.2% PES (red) shown alongside the additive concentration remaining (right y-axis). Cells were charged at a current of C/20 and 40 °C. (For interpretation of the references to colour in this figure legend, the reader is referred to the web version of this article.)

concentration originally put in the cells. Fig. 1 shows that the concentrations of additives measured from cells that were not charged were 2.1% for both VC and PES-containing cells. This indicates that the extraction method does not cause any significant loss of additive.

Generally, the consumption profile of PES during the first charge is very similar to that for VC. That is, the largest concentration drop occurs between 1.5 V and 3.0 V as the cell is charged. This is expected since in this potential range the graphite electrode potential drops below the reduction potential of the additives. Based on the assumption that the reduction of the additive leads to the formation of a passivating layer, one would expect that the rate of consumption of the additive would dramatically slow past this 1.5–3 V range. However, Fig. 1 clearly shows that both VC and PES continue reacting in a significant manner past the peak corresponding to their electrochemical reduction. This sustained consumption may originate from an incomplete graphite passivation (partial passivation), or from the reaction between the remaining additive and nucleophilic by-products commonly generated during reductive processes [18,27–31]. The main difference between PES and VC seems to be that PES consumption slows down significantly between 3.5 V and 3.75 V (no significant consumption) while VC consumption still occurs. Fig. 1 clearly shows that the reduction peak of the additive in the differential capacity vs. potential plot during the first charge of a cell (formation cycle) only partially reflects the reactivity of an additive.

Fig. 2 shows the amount of PES consumed (a) and the magnitude of the impedance ( $R_{ct}$ ) (b) as a function of initial PES loading after the first cycle of NMC(111)/graphite pouch cells. Here  $R_{ct}$  is defined as the real impedance difference between the two negative imaginary minima of the Nyquist plot of the impedance.  $R_{ct}$  then

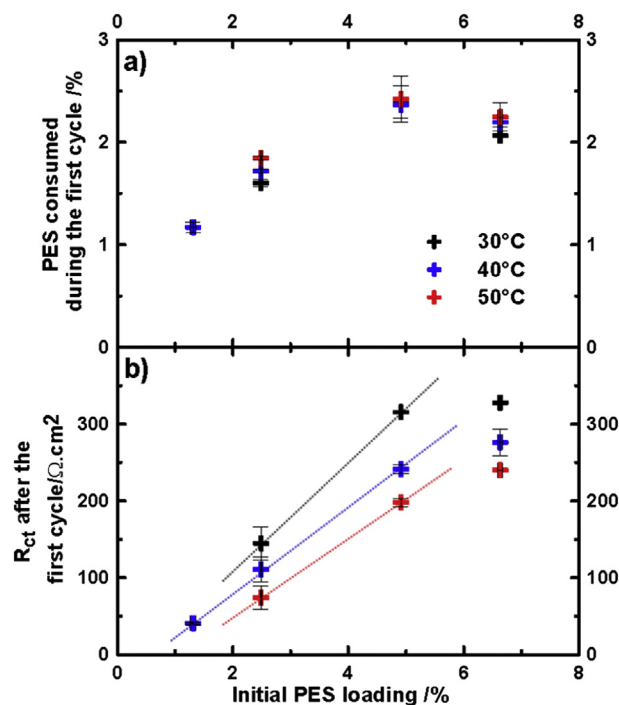


**Fig. 2.** Amount of PES consumed (a) and  $R_{ct}$  (see text for the definition of  $R_{ct}$ ) (b) as a function of initial PES loading for NMC(111)/graphite cells that underwent 1 full cycle at C/20 and various temperatures. Cells were charged at a current of C/20 and 40 °C. The impedance spectra used to determine the value of  $R_{ct}$  were measured at 3.80 V during the first discharge. Dotted lines have been fitted through the  $R_{ct}$  of cells with initial PES loading from 1% to 5% to highlight the non-linear impedance rise at higher initial PES loading.

encompasses the contact resistance between the current collector and active particles, the diffusion of  $\text{Li}^+$  through the pores of the electrode, the desolvation of  $\text{Li}^+$  as well as the resistance to the transfer of  $\text{Li}^+$  through the SEI [21,32–34]. Fig. 2a shows that the amount of PES consumed during the first cycle increases with initial PES loading between 1 and 5% and then seems to level at an initial PES loading higher than 5%. This trend was observed for all formation temperatures tested.

Fig. 2b shows that the magnitude of the impedance of cells after the first cycle follows a similar trend as the additive consumption. That is,  $R_{ct}$  increases with increasing initial PES loading between 1 and 5% and then increases to a lesser extent at higher initial loadings. Fig. 2b suggests that the impedance of cells initially containing PES is dependent upon the amount of additive that has reacted. Petibon et al. found similar trend between the amount of VC consumed and the magnitude of the impedance of NMC(111)/graphite cells [7]. Fig. 2b also shows that for the same initial PES loading, cells formed at higher temperature have lower impedance. It is possible that different formation temperature yields different SEI composition as previously suggested by Pinson et al. [35]. It is also possible that temperature effect on impedance might be related to an accelerated SEI aging effect. For instance, Xia et al. [11] and Nelson et al. [13] showed that the impedance of cells containing PES was smaller after cycling and storage than after the formation cycle.

### 3.2. Consumption during hold periods

In order to assess whether PES was consumed at the positive electrode during cell use, the concentration of PES remaining after holding NMC(111)/graphite cells at two different potentials was measured. Fig. 3a shows the cell potential vs. time profile of NMC(111)/graphite cells prior to additive concentration measurements. Fig. 3a shows that cells underwent an initial full charge to an upper cut-off of 4.2 V. Cells were then discharged to 3.8 V and finally charged to their respective hold-potentials. Some cells were held at 3.9 V for 250 h while others were held for the same period of time at 4.2 V. With the specific positive electrode and negative electrode active mass ratio of the cell type used, at a cell potential of 3.9 V and 4.2 V, the graphite electrode is in a two-phase region and its potential vs.  $\text{Li}/\text{Li}^+$  is constant at about 73 mV vs  $\text{Li}/\text{Li}^+$  [36,37]. By contrast, the positive electrode potential changes significantly (3.97 V vs.  $\text{Li}/\text{Li}^+$  and 4.27 V vs.  $\text{Li}/\text{Li}^+$  respectively). As a consequence, any difference in the amount of PES consumed during the potential-hold at 3.9 V and 4.2 V would suggest that PES reacts at the positive electrode (at 4.27 V vs.  $\text{Li}/\text{Li}^+$  at least) in a quantifiable manner.

Fig. 3b and c shows the amount of PES consumed during the 250 h hold in cells initially containing 2.5% PES (3b) and 4.5% PES (3c). The experiment was performed at both 40 °C (blue) and 50 °C (red). Fig. 3b and c clearly show that cells held at 4.2 V have more PES consumed during the hold than cells held at 3.9 V, for both cells initially containing 2.5% and 4.5% PES at both temperatures. This suggests that PES reacts at the positive electrode at 4.27 V vs.  $\text{Li}/\text{Li}^+$  in a quantifiable manner or that the reaction at the negative electrode is accelerated by a higher potential positive electrode in some manner. Since Madec et al. [27] showed X-ray photoelectron spectroscopy data strongly suggesting that PES reacts at the positive electrode, the former possibility is considered below.

In a recent publication Self et al. [28] presented the results of density function theory (DFT) calculations on PES oxidation. Their results indicated that the oxidation of PES is unlikely to be caused by direct electron transfer. They indicated that PES is likely to react at the positive electrode surface of partially delithiated layered materials following what they called the “reactive electrode

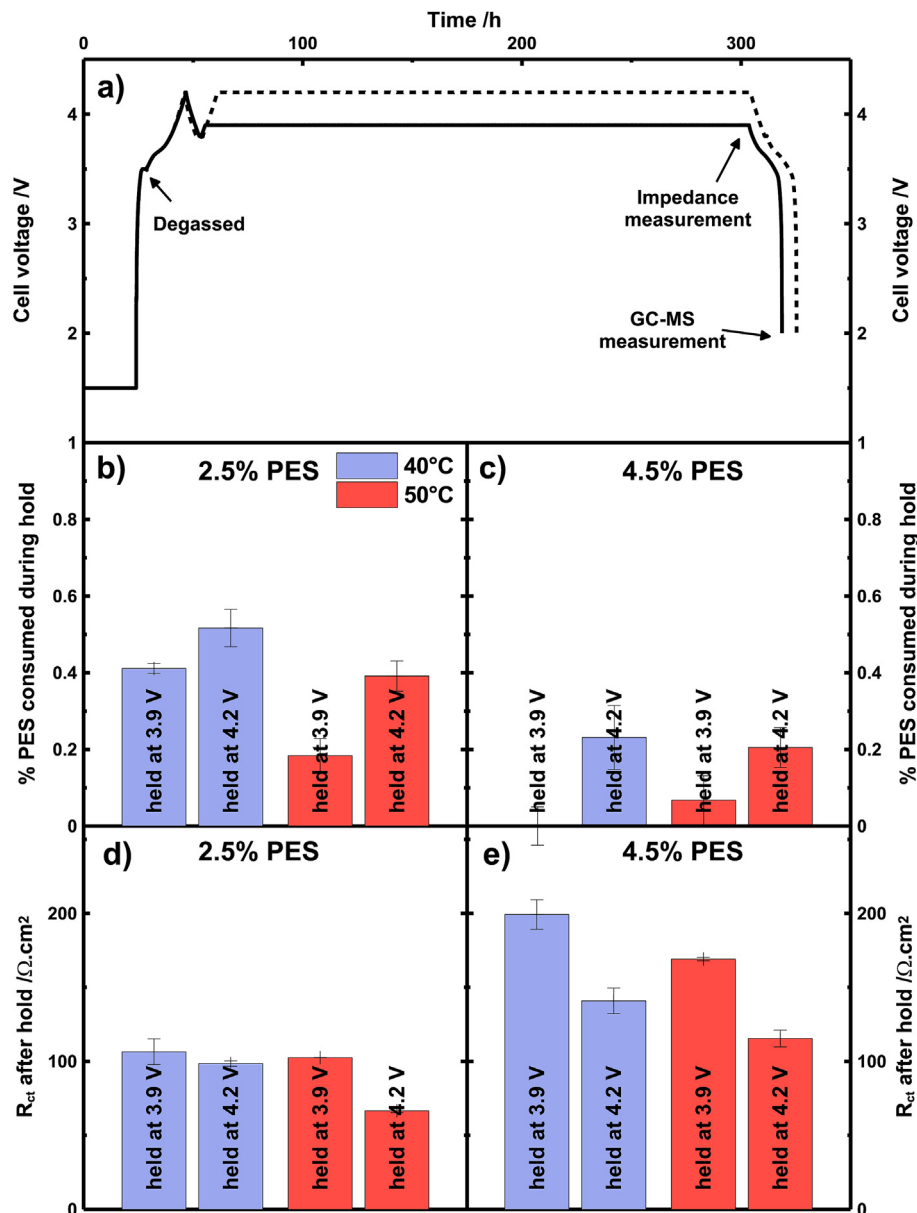
model”. In this model the oxidation goes through an oxygen transfer from the partially delithiated  $\text{Li}_x\text{MO}_2$  (where M is Ni, Mn, or Co) positive electrode surface to PES in a “pseudo combustion reaction”. The reaction could result in the formation of a rock salt layer ( $\text{MO}$ , where M is Ni, Mn, Co) at the electrode surface and various organic by-products. Rocksalt surface layers have been observed in a number of literature papers [38–41]. The calculated by-products included carbonyl sulfide, ethene, and organosulfur compounds, all of which were identified experimentally by Self et al. [42]. The results presented in Fig. 3b and c suggest that this reaction may occur at 4.27 V vs.  $\text{Li}/\text{Li}^+$  with NMC(111) electrodes. This also suggests that PES can alter the passivation layer at the positive electrode.

Fig. 3b and c also show that while the consumption of PES during the hold at 3.9 V is quantifiable in cells with a starting concentration of 2.5%, almost no PES is consumed in cells initially containing 4.5% PES. This seems to indicate that the passivation of the graphite surface in the presence of PES is more effective at higher initial PES concentration. This might explain the apparent break in the PES consumption trend with initial loading seen in Fig. 2a. Fig. 3b and c shows that the effect of temperature on PES consumption is not obvious. For instance, Fig. 3b shows that PES consumption in cells initially containing 2.5% PES is lower at 50 °C than at 40 °C while in cells initially containing 4.5% PES, the consumption is slightly higher at 50 °C than at 40 °C.

Fig. 3d and e shows  $R_{ct}$  of cells initially containing 2.5% PES (3d) and 4.5% PES (3e) after the potential-hold periods. Fig. S4 shows the measured Nyquist spectra for interested readers. Fig. 3d and e shows that  $R_{ct}$  of cells held at 4.2 V is consistently lower than the impedance of cells held at 3.9 V. Fig. 3d and e also show that the impedance of cells held at 50 °C is generally lower than the impedance of cells held at 40 °C. It then seems that the reduction of impedance during cycling observed by Xia et al. [11] Nelson et al. [13] in cells containing PES originates from the positive electrode and is more pronounced at elevated temperature. In order to determine the impedance of the graphite electrode and of the NMC(111) electrode after the holds at 3.9 V and 4.2 V, symmetric cells were reconstructed from the NMC(111)/graphite pouch cells.

### 3.3. Impedance of individual electrodes

Fig. 4 shows the Nyquist plot of the impedance of positive symmetric cells reconstructed from NMC(111)/graphite pouch cells initially containing no additive (a), 2.5% PES (b) and 4.5% PES (c) after the first cycle (black), after a 250 h hold at 3.9 V (blue) and after a 250 h hold at 4.2 V (red). The impedance of the symmetric cells was divided by two in order to present the impedance of a single electrode. Fig. 4 shows that the Nyquist plots of the impedance of positive symmetric cells present two features. The feature at high frequency is due to the contact resistance between the current collector and the active particles [21,23,32] as well as the contact resistance between the coin cell can and the back side of the electrode. In full pouch cells cycled at moderate voltages (<4.3 V), the contribution of the contact resistance between the current collector and the active material is negligible. This can be seen from the absence of any pronounced high frequency feature in the impedance spectra of the full pouch cells presented in Fig. S4. This feature is a lot larger in the reconstructed positive symmetric cells than in the full pouch cell since the symmetric cells have an added interface between the can of the coin cell and the back of the electrode. The high frequency feature in Fig. 4 can then be ignored. The discussion below will only deal with the medium frequency feature. The feature at medium frequency of the impedance spectra of the positive symmetric cells corresponds to the  $\text{Li}^+$  desolvation,  $\text{Li}^+$  transfer through the SEI as well as the charge transfer resistance



**Fig. 3.** Cell voltage vs. time profile of the hold experiments (a), amount of PES consumed during the hold period (between the start of the hold and the end of the hold) (b, c), and  $R_{ct}$  (see text for the definition of  $R_{ct}$ ) after the hold period (d, e) in NMC(111)/graphite cells initially containing 2.5% PES (b, d), and 4.5% PES (c, e). All impedance spectra were measured at 10 °C and 3.8 V.

of the electron and  $\text{Li}^+$  across the active particle interface [21,22,32,33]. Fig. 4 shows that the positive electrode impedance of cells containing PES undergoes little change between the formation cycle, 250 h hold at 3.9 V and 250 h hold at 4.2 V. To put things into perspective,  $R_{ct}$  of the full cell containing 2.5% PES was around  $100 \Omega \text{ cm}^2$  after the 3.9 V hold (see Fig. 3d) while  $R_{ct}$  of the positive electrode (ignoring the contact resistance of the symmetric cell) is around  $15 \Omega \text{ cm}^2$  in Fig. 4b.

Fig. 5 shows the Nyquist plot of the impedance of negative symmetric cells reconstructed from the same NMC(111)/graphite pouch cells used in Fig. 4. Fig. 5 shows that the impedance of the negative electrode of all pouch cells containing PES changed significantly between the first cycle and different holds. Fig. 5 shows that the impedance of cells containing PES is lower after the 4.2 V hold than after the 3.9 V hold. This is surprising since at these two full cell voltages, the graphite electrode potential (vs. Li/

$\text{Li}^+$ ) does not change significantly. The readers are reminded that all symmetric cells were reconstructed after the pouch cells were equilibrated at a full cell voltage of 3.8 V. Bringing all cells to the same voltage before opening was done to ensure that the differences seen in the impedance of each electrode come from the composition of the SEI or changes in SEI structure and not from electrochemical potential differences. Figs. 4 and 5 clearly show that the lower full cell impedance of PES-containing cells held at 4.2 V seen in Fig. 3 originates from lower negative electrode impedance after the potential hold. The fact that between 3.9 V and 4.2 V only the positive electrode potential changes strongly suggests a positive-negative electrode interaction. These types of interactions have now been reported by several researchers. For instance, Burns et al. showed clear evidence of deposit on the graphite electrode originating from the positive electrode in NMC(111)/graphite 18650 type cells tested to a cut-off potential of

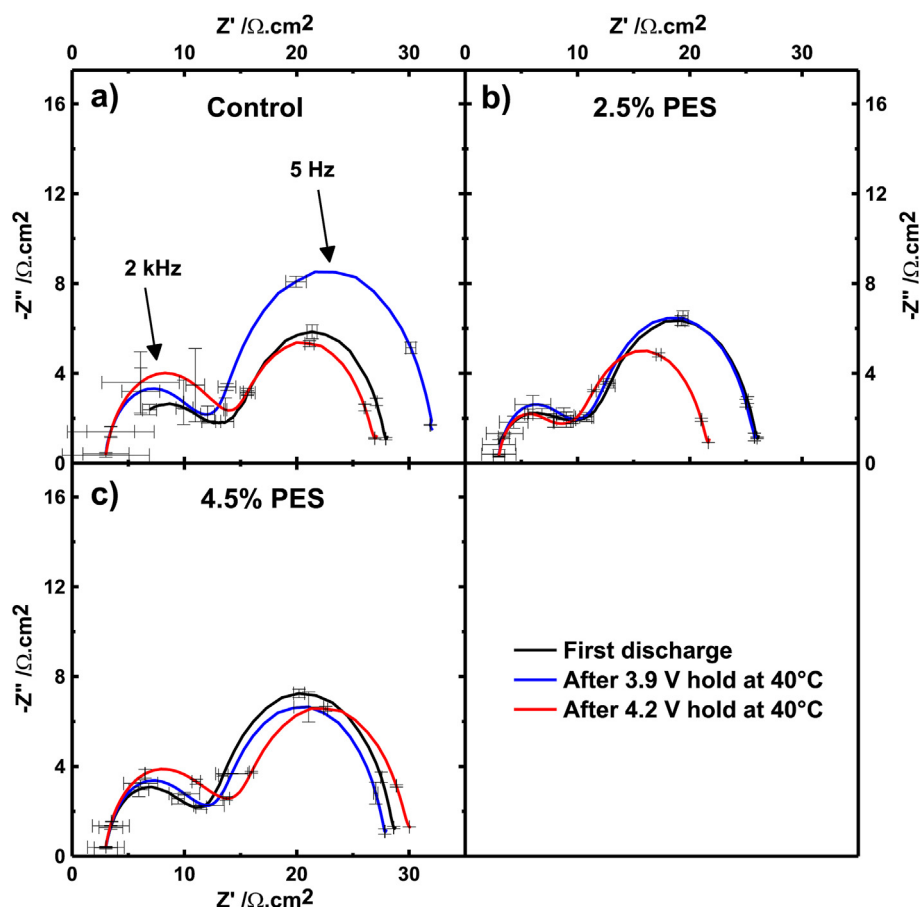


**Fig. 4.** Area specific negative imaginary part of the impedance as a function of the area specific real part of the impedance of the positive electrode of NMC(111)/graphite cells filled with a control electrolyte (a), with an electrolyte initially containing 2.5% PES (b) and 4.5% PES (c), after the first discharge (black), after a 250 h hold at 3.9 V (blue) and after a 250 h hold at 4.2 V (red). All symmetric cells were reconstructed from pouch cells equilibrated at 3.8 V. All impedance spectra were measured at 10 °C. (For interpretation of the references to colour in this figure legend, the reader is referred to the web version of this article.)

4.2 V [43]. In a similar manner, Jarry et al. showed clear evidence of the deposition of fluorescent organometallic compounds at the surface of the graphite electrode originating from the positive electrode of  $\text{Li}_x\text{Ni}_{0.5}\text{Mn}_{1.5}\text{O}_{4-\delta}$ /graphite cells tested to a cutoff potential of 4.85 V [44]. Li et al. also reported clear evidence for a positive-negative electrode interaction in  $\text{LiNi}_{0.5}\text{Mn}_{1.5}\text{O}_4/\text{Li}_4\text{Ti}_5\text{O}_{12}$  cells tested to 5.0 V vs.  $\text{Li}/\text{Li}^+$  [45]. Figs. 3–5 clearly show that these interactions have a large impact on the surface of the negative electrode.

Comparing the impedance spectra of the positive electrode and negative electrode of cells containing no additive, 2.5% PES and 4.5% PES after the first cycle helps explain the impedance growth seen in cells with increased initial PES loading (Fig. 2b). Figs. 4 and 5 indicate that while the impedance of the positive electrode of all cells does not change significantly with PES loading, the impedance of the negative electrode changes dramatically. This means that the increase in impedance associated with the increase in initial PES loading originates from an increase of the impedance of the negative electrode. The effect of PES on the negative electrode impedance is very similar to the effect of VC as reported by Burns et al. [25] and Petibon et al. [26].

#### 3.4. Schematics of the surface composition of the electrodes

Fig. 6 shows a schematic of the SEI formed at the negative electrode of NMC(111)/graphite pouch cells containing no additives

(control), initially containing 2.5% PES and initially containing 4.5% PES after a 250 h hold at 3.9 V and after a 250 h hold at 4.2 V. Table 1 also shows the detailed atomic percentages (at. %) obtained from XPS quantification. The composition of the SEI was determined using the analysis of C 1s, O 1s, F 1s and P 2p XPS core spectra of the surface of the graphite electrodes from the appropriate cells. The XPS core spectra used for this analysis along with their descriptions and the fitting procedure used are presented in the [supplementary information](#).

Fig. 6 and Table 1 show that the SEI at the negative electrode of cells held at 4.2 V is quite different than that of cells held at 3.9 V (the thicknesses were evaluated to be 10–14 nm). This again suggests the presence of an interaction between the positive electrode and the negative electrode since only the potential of the positive electrode changes significantly. The SEI at the negative electrode of cells held at 4.2 V is thicker independently of the composition of the electrolyte. Fig. 6 and Table 1 show that the SEI of the negative electrode of cells containing no additive is mostly composed of LiF as well as polyethylene oxide and hemicarbonates after the 3.9 V hold. The SEI of cells containing no additive after the 4.2 V holds is thicker and mostly composed of LiF. Fig. 6 and Table 1 show that the difference in thickness of the negative electrode SEI in cells containing PES at 3.9 V and at 4.2 V is a lot smaller than that of cells containing no additive. This is consistent with a lower parasitic oxidation rate observed in cells containing PES. Since the parasitic oxidation rate is smaller, fewer by-products migrate to the negative

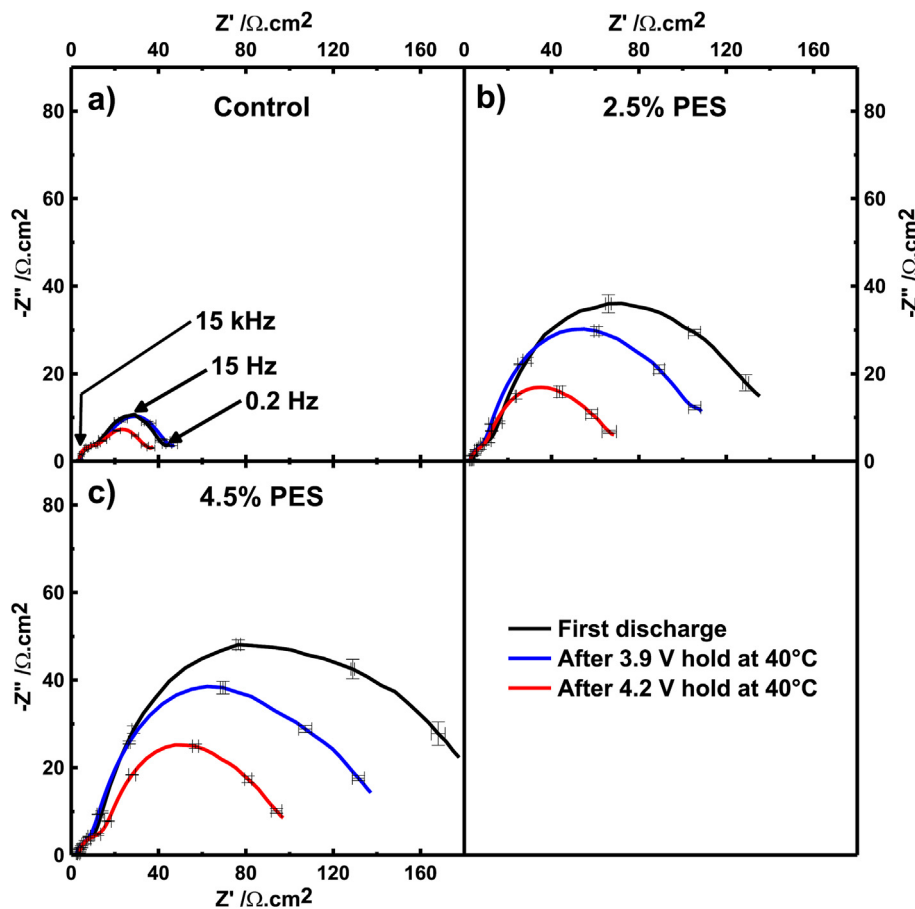


**Fig. 5.** Area specific negative imaginary part of the impedance as a function of the area specific real part of the impedance of the negative electrode of NMC(111)/graphite cells filled with a control electrolyte (a), with an electrolyte initially containing 2.5% PES (b), and 4.5% PES (c), after the first discharge (black), after a 250 h hold at 3.9 V (blue) and after a 250 h hold at 4.2 V (red). All symmetric cells were reconstructed from pouch cells equilibrated at 3.8 V. All impedance spectra were measured at 10 °C. (For interpretation of the references to colour in this figure legend, the reader is referred to the web version of this article.)

electrode. Fig. 6 and Table 1 also show that the composition of the negative electrode SEI in cells containing PES is a lot different than in the case of cells containing no additive. Fig. 6 shows that the SEI of cells containing PES is mostly composed of organic and organosulfur compounds. This is very different from the mostly inorganic SEI observed in cells containing no additive. For a more detailed analysis of the SEI at the electrode of cells containing PES in EC-based electrolytes, readers are invited to consult the recent publication by Madec et al. [12].

Fig. 7 shows a schematic of the SEI at the positive electrode of NMC(111)/graphite pouch cells containing no additive, initially containing 2.5% PES and 4.5% PES after a 250 h hold at 3.9 V and after a 250 h hold at 4.2 V. Table 2 also shows the detailed atomic percentages (at. %) obtained from XPS quantification. Again, the composition of the SEI was determined using C 1s, O1s, F 1s, and P 2p XPS core spectra. These XPS core spectra as well as their analysis can be found in the supplementary information. Fig. 7 and Table 2 show that the SEI at the positive electrode of all cells held at 4.2 V is thicker than that of cells held at 3.9 V (the thicknesses were evaluated to be 1–4 nm, see Table 2). Fig. 7 and Table 2 also show that the SEI thickness difference after the 3.9 V hold and the 4.2 V hold is greater for cells initially containing 4.5% PES than for cells initially containing 2.5% PES. Fig. 7 and Table 2 also show that in general, cells containing PES have a thicker SEI at the positive electrode than cells without additive. The SEI of the positive electrodes in cells initially containing PES also contains a significant amount of

organosulfur compounds. These two differences may be the origin of the lower parasitic current rate at the positive electrode in cells initially containing PES as suggested by Madec et al. [12]. Again, a detailed analysis of the SEI is beyond the scope of this paper and the readers are invited to consult the result publication by Madec et al. [12].

#### 4. Conclusions

The consumption of PES in NMC(111)/graphite cells during formation and after 250 h holds at different potentials was measured using the GC-MS procedure described by Petibon et al. [17]. The PES concentration vs. cell voltage profile during the formation charge indicated that a significant portion of PES is consumed after the reduction peak in the differential capacity plot. This indicates that relying on the differential capacity peak to assess the reactivity of one additive may give an incomplete picture. This was very similar to the results presented by Petibon et al. about the consumption of VC during the formation charge of NMC(111)/graphite pouch cells [7]. This added consumption may originate from further electrochemical reduction of the additive, or the reaction of PES with other by-products.

GC-MS measurements of the electrolyte in cells that underwent one full cycle indicated that the amount of PES consumed increases with initial additive loading between 1 and 5% and then levels at higher initial loading. The reason for this trend change remains

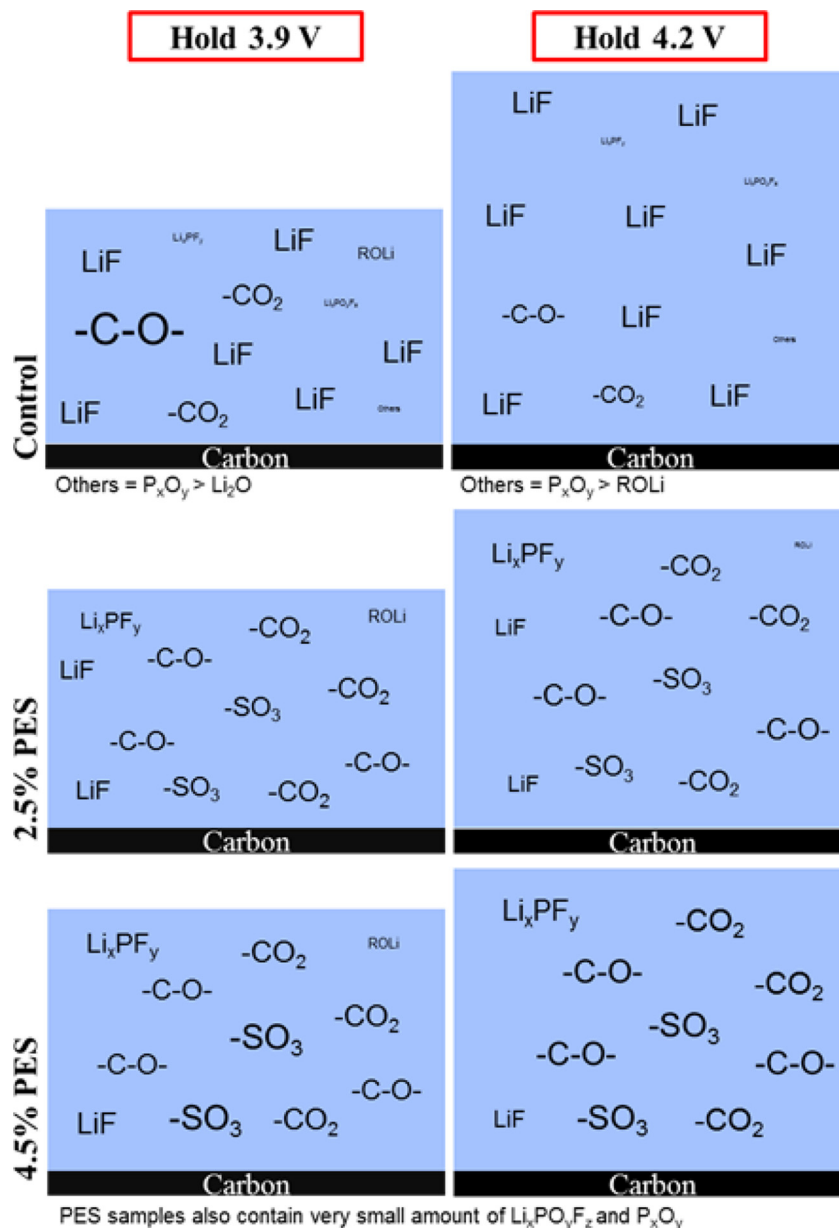


**Fig. 6.** Schematic representations of the SEI on the lithiated graphite electrodes taken from NMC(111)/graphite pouch cells initially containing no additive (control), 2.5% PES and 4.5% PES after a 250 h hold at 3.9 V and 40 °C and after a 250 h hold at 4.2 V and 40 °C, as deduced from the XPS experiments (the XPS core spectra can be found in the [supplementary information](#)). The heights of the SEI films at the graphite surface in Fig. 6 are proportional to their true heights. The size of the fonts reflects the abundance of the species.

unknown and may relate to a more complete passivation of the graphite at higher PES loading. EIS measurements of cells that underwent one full cycle indicated that the magnitude of the impedance increased as the PES consumption increased. EIS on symmetric cells later showed that this impedance increase originated from the graphite electrode.

NMC(111)/graphite cells were held at two different potentials, where only the positive electrode potential changed, to assess whether PES was directly consumed at the positive electrode. The experiment showed the existence of a positive-negative electrode interaction. The quantification of the additive remaining in the cells after the holds at the two different potentials showed that PES must react at the positive electrode more rapidly at higher potential. DFT calculations presented by Self et al. [28] suggested that this consumption can possibly happen through a “reactive electrode”

mechanism. In this proposed mechanism, the delithiated NMC(111) surface reacts with PES yielding a rock salt structure at the surface of the electrode, as well as carbonyl sulfide and organosulfur by-products.

EIS on symmetric cells as well as XPS showed that the negative electrode surface of NMC(111)/graphite cells after a 250 h period at 4.2 V differs from the negative electrode surface of cells held at 3.9 V. This was surprising since the electrochemical potential of the graphite electrode does not change when the cells are at 3.9 V or at 4.2 V. Fig. 8 presents a schematic of the mechanism that is likely to explain this phenomenon in cells containing no additive (top) and cells containing PES (bottom). Fig. 8 shows that at 3.9 V, components of the electrolyte (S) are oxidized at the positive electrode yielding a by-product “P<sup>+</sup>” (the electron transfer and Li<sup>+</sup> transfer are omitted on this schematic for clarity). Some of these by-

**Table 1**  
Atomic percentages (at. %) obtained from XPS quantification for graphite electrodes as taken from NMC/graphite pouch cells with control, 2.5% PES and 4.5% electrolytes after potential hold during 250 h at 3.9 V and 4.2 V.

		B.E. (eV)	Control 3.9 V	Control 4.2 V	2.5% PES 3.9 V	2.5% PES 4.2 V	4.5% PES 3.9 V	4.5% PES 4.2 V
F 1s	LiF	685–685.3	19.6	31.5	3.5	3.2	1.8	1.4
	Li <sub>x</sub> PF <sub>y</sub> /Li <sub>x</sub> PO <sub>y</sub> F <sub>z</sub>	687–687.5	10.4	10.2	13.0	15.1	13.5	13.5
	<b>SUM (%)</b>		<b>29.9</b>	<b>41.7</b>	<b>16.5</b>	<b>18.3</b>	<b>15.3</b>	<b>14.9</b>
O 1s	CO <sub>2</sub> /SO <sub>3</sub>	532	8.3	5.7	16.9	17.9	18.6	18.7
	CO	533.8	4.8	3.2	5.4	6.2	5.2	5.9
	ROLi	530.3	0.8	0.3	1.2	0.5	0.8	0.1
	Li <sub>2</sub> O	528.3	0.3	–	–	–	–	–
	<b>SUM (%)</b>		<b>14.2</b>	<b>9.2</b>	<b>23.4</b>	<b>24.6</b>	<b>24.7</b>	<b>24.7</b>
C 1s	C=C	282.7	1.0	0.1	1.3	0.4	1.0	0.5
	CH	285	19.8	7.8	27.8	24.9	29.3	30.5
	CO	286.7	5.9	3.3	8.7	9.8	9.9	9.8
	CO <sub>2</sub>	289.3	1.5	0.9	2.2	2.5	1.9	2.4
	CO <sub>3</sub>	290.7	1.1	0.4	0.9	0.9	0.5	0.8
	<b>SUM (%)</b>		<b>29.3</b>	<b>12.5</b>	<b>40.9</b>	<b>38.5</b>	<b>42.4</b>	<b>44.1</b>
P 2p	P <sub>x</sub> O <sub>y</sub>	133.7134.6	0.4	0.4	0.1	0.1	0.0	0.0
	Li <sub>x</sub> PO <sub>y</sub> F <sub>z</sub>	135,135.9	1.0	1.1	0.1	0.2	0.1	0.2
	Li <sub>x</sub> PF <sub>y</sub>	137,137.9	1.2	1.0	1.5	1.9	1.7	1.8
	<b>SUM (%)</b>		<b>2.6</b>	<b>2.6</b>	<b>1.7</b>	<b>2.2</b>	<b>1.9</b>	<b>2.0</b>
Li 1s		55	24.0	34.1	13.9	12.5	11.5	10.2
S 2p	RSO <sub>3</sub> Li	168.8170	–	–	3.0	3.5	3.8	3.9
	Li <sub>2</sub> SO <sub>3</sub>	167,168.2	–	–	0.6	0.4	0.5	0.3
	<b>SUM (%)</b>				<b>3.6</b>	<b>3.9</b>	<b>4.3</b>	<b>4.2</b>
<b>Estimated thickness</b>			<b>9.8 nm</b>	<b>15.6 nm</b>	<b>10 nm</b>	<b>13.3 nm</b>	<b>11.0 nm</b>	<b>12.7 nm</b>

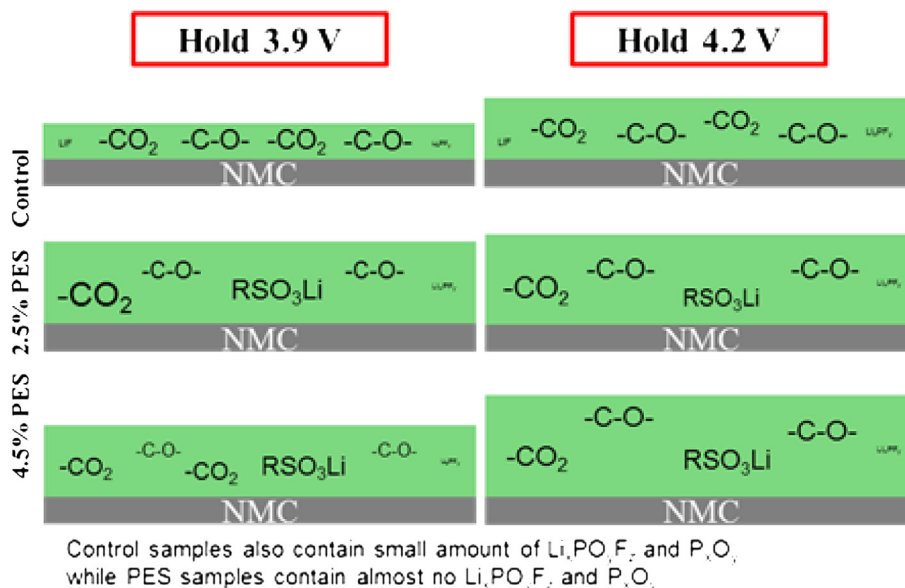


**Fig. 7.** Schematic representations of the SEI films on the delithiated NMC(111) electrodes taken from NMC(111)/graphite pouch cells initially containing no additive (control), 2.5% PES and 4.5% PES after a 250 h hold at 3.9 V and 40 °C and after a 250 h hold at 4.2 V and 40 °C, as deduced from the XPS experiments (the XPS core spectra can be found in the [supplementary information](#)). The heights of the SEI films at the NMC surface in [Fig. 7](#) are proportional to their true heights. The size of the fonts reflects the abundance of the specie.

products may travel through the electrolyte and reach the negative electrode. The by-products may then diffuse through the SEI and approach the graphite surface within the electron tunneling distance. At this point, the by-products of the oxidation of the electrolyte are reduced and integrated in the SEI of the negative electrode. At 3.9 V, the flux of oxidation by-products is small due to the low potential of the positive electrode. The changes in the SEI of the negative electrode observed between cell formation and the hold at 3.9 V, as seen in the impedance spectra presented in [Fig. 5](#), are believed to come from the direct reduction of the electrolyte at the negative electrode. At 4.2 V, the oxidation rate of the electrolyte at the positive electrode increases. A higher flux of oxidation by-products reaches the negative electrode and is reduced there. The

increased oxidation rate may then result in an increased SEI thickness at the negative electrode as observed by XPS. The reduction of the oxidation by-products modifies the composition and morphology of the SEI at the negative electrode. This ultimately leads to a change in the impedance of the negative electrode as observed using EIS on symmetric cells. In cells initially containing PES, the electrolyte oxidation rate is smaller than in cells containing no additives [11]. As a result, the flux of by-products going from the positive electrode to the negative electrode is smaller than in cells containing no additive. This flux of by-products is nonetheless high enough to modify the SEI at the negative electrode as can be seen in the impedance spectra of the negative electrodes presented in [Fig. 5](#). The results presented here clearly show that these

**Table 2**

Atomic percentages (at. %) obtained from XPS quantification for NMC electrodes as taken from NMC/graphite pouch cells with control, 2.5% PES and 4.5% electrolytes after potential hold during 250 h at 3.9 V and 4.2 V.

		B.E. (eV)	Control 3.9 V	Control 4.2 V	2.5% PES 3.9 V	2.5% PES 4.2 V	4.5% PES 3.9 V	4.5% PES 4.2 V
F 1s	CF (PVdF)	687.2	19.2	18.6	16.4	20.3	18.8	17.4
	LiF	684.2	0.6	0.6	0.3	0.4	0.3	0.1
	unknown	685.8	1.8	3.2	1.9	1.6	1.9	2.2
	<b>SUM (%)</b>		<b>21.7</b>	<b>22.3</b>	<b>18.5</b>	<b>22.3</b>	<b>21.0</b>	<b>19.8</b>
O 1s	Lattice O <sub>2</sub>	529.5	6.6	4.2	2.9	2.5	3.5	2.0
	CO <sub>2</sub> , SO <sub>3</sub>	531.9	9.5	10.4	16.5	15.1	17.4	15.5
	CO	533.7	5.2	7.6	6.1	7.3	4.5	7.4
	<b>SUM (%)</b>		<b>21.2</b>	<b>22.2</b>	<b>25.4</b>	<b>24.9</b>	<b>25.3</b>	<b>24.9</b>
C 1s	C=C (carbon)	284.6	26.9	20.2	24.0	15.0	20.2	17.1
	CH/CO <sub>x</sub>	285–290	21.5	26.6	22.2	26.6	24.2	28.2
	CF (PVdF)	290.3	8.2	7.5	5.6	7.2	5.8	5.5
	<b>SUM (%)</b>	290.7	<b>56.6</b>	<b>54.4</b>	<b>51.8</b>	<b>48.7</b>	<b>50.2</b>	<b>50.9</b>
P 2p	P <sub>x</sub> O <sub>y</sub>	133.7134.6	0.1	0.2	0.0	0.1	0.0	0.0
	Li <sub>x</sub> PO <sub>y</sub> F <sub>z</sub>	134.9135.8	0.0	0.2	0.2	0.2	0.2	0.2
	Li <sub>x</sub> PF <sub>y</sub>	136.7137.6	0.3	0.8	0.8	0.9	0.6	1.0
	<b>SUM (%)</b>		<b>0.5</b>	<b>1.1</b>	<b>1.1</b>	<b>1.2</b>	<b>0.8</b>	<b>1.2</b>
S 2p	RSO <sub>3</sub> Li	168.6169.8			3.2	2.9	2.7	3.3
	<b>Estimated thickness</b>		<b>1.4 nm</b>	<b>2.3 nm</b>	<b>3.1 nm</b>	<b>3.4 nm</b>	<b>2.7 nm</b>	<b>3.9 nm</b>

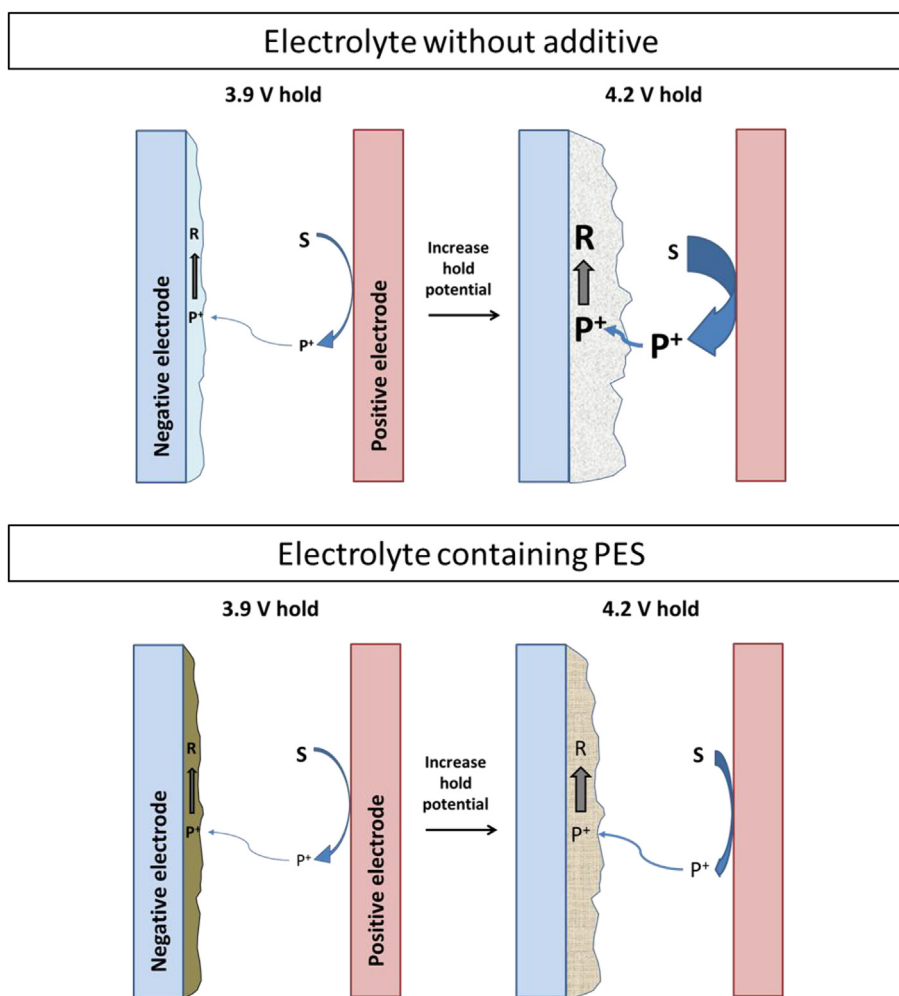


Fig. 8. Schematic of the interaction between the positive electrode and the negative electrode and its dependence on cell voltage.

interactions need to be understood in order to have a complete understanding of the evolution of the SEI at both electrodes. It also shows that the SEI of the graphite electrode in cells operated at high

voltage may be greatly affected by high fluxes of oxidation by-products.

## Acknowledgments

The authors would like to thank 3M Canada and NSERC for the partial funding of this work. The authors thank Dr. Jing Li of BASF for providing some of the solvents, salts and additives used in his work. Remi Petibon thanks NSERC and the Walter C. Sumner Foundation for Scholarship support.

## Appendix A. Supplementary data

Supplementary data related to this article can be found at <http://dx.doi.org/10.1016/j.jpowsour.2016.02.054>.

## References

- [1] D. Aurbach, K. Gamolsky, B. Markovsky, Y. Gofer, M. Schmidt, U. Heider, On the use of vinylene carbonate (VC) as an additive to electrolyte solutions for Li-ion batteries, *Electrochim. Acta* 47 (2002) 1423–1439, [http://dx.doi.org/10.1016/S0013-4686\(01\)00858-1](http://dx.doi.org/10.1016/S0013-4686(01)00858-1).
- [2] D.Y. Wang, N.N. Sinha, R. Petibon, J.C. Burns, J.R. Dahn, A systematic study of well-known electrolyte additives in LiCoO<sub>2</sub>/graphite pouch cells, *J. Power Sources* 251 (2014) 311–318, <http://dx.doi.org/10.1016/j.jpowsour.2013.11.064>.
- [3] D.Y. Wang, J. Xia, L. Ma, K.J. Nelson, J.E. Harlow, D. Xiong, et al., A systematic study of electrolyte additives in Li[Ni<sub>1</sub>/3Mn<sub>1</sub>/3Co<sub>1</sub>/3]O<sub>2</sub> (NMC)/graphite pouch cells, *J. Electrochem. Soc.* 161 (2014) A1818–A1827, <http://dx.doi.org/10.1149/2.0511412jes>.
- [4] J.-Y. Eom, I.-H. Jung, J.-H. Lee, Effects of vinylene carbonate on high temperature storage of high voltage Li-ion batteries, *J. Power Sources* 196 (2011) 9810–9814, <http://dx.doi.org/10.1016/j.jpowsour.2011.06.095>.
- [5] H. Ota, Y. Sakata, A. Inoue, S. Yamaguchi, Analysis of vinylene carbonate derived SEI layers on graphite anode, *J. Electrochem. Soc.* 151 (2004) A1659–A1669, <http://dx.doi.org/10.1149/1.1785795>.
- [6] L.E. Ouatani, R. Dedryvère, C. Siret, P. Biensan, S. Reynaud, P. Iratçabal, et al., The effect of vinylene carbonate additive on surface film formation on both electrodes in Li-ion batteries, *J. Electrochem. Soc.* 156 (2009) A103–A113, <http://dx.doi.org/10.1149/1.3029674>.
- [7] R. Petibon, J. Xia, J.C. Burns, J.R. Dahn, Study of the consumption of vinylene carbonate in Li[Ni<sub>0.33</sub>Mn<sub>0.33</sub>Co<sub>0.33</sub>]O<sub>2</sub>/graphite pouch cells, *J. Electrochem. Soc.* 161 (2014) A1618–A1624, <http://dx.doi.org/10.1149/2.0351410jes>.
- [8] J.C. Burns, N.N. Sinha, D.J. Coyle, G. Jain, C.M. VanElzen, W.M. Lamanna, et al., The impact of varying the concentration of vinylene carbonate electrolyte additive in wound Li-ion cells, *J. Electrochem. Soc.* 159 (2011) A85–A90, <http://dx.doi.org/10.1149/2.028202jes>.
- [9] B. Li, M. Xu, T. Li, W. Li, S. Hu, Prop-1-ene-1,3-sultone as SEI formation additive in propylene carbonate-based electrolyte for lithium ion batteries, *Electrochim. Commun.* 17 (2012) 92–95, <http://dx.doi.org/10.1016/j.elecom.2012.02.016>.
- [10] B. Li, M. Xu, B. Li, Y. Liu, L. Yang, W. Li, et al., Properties of solid electrolyte interphase formed by prop-1-ene-1,3-sultone on graphite anode of Li-ion batteries, *Electrochim. Acta* 105 (2013) 1–6, <http://dx.doi.org/10.1016/j.electacta.2013.04.142>.
- [11] J. Xia, L. Ma, C.P. Aiken, K.J. Nelson, L.P. Chen, J.R. Dahn, Comparative study on prop-1-ene-1,3-sultone and vinylene carbonate as electrolyte additives for Li(Ni<sub>1</sub>/3Mn<sub>1</sub>/3Co<sub>1</sub>/3)O<sub>2</sub>/graphite pouch cells, *J. Electrochem. Soc.* 161 (2014) A1634–A1641, <http://dx.doi.org/10.1149/2.0541410jes>.
- [12] L. Madec, R. Petibon, J. Xia, J.-P. Sun, I.G. Hill, J.R. Dahn, Understanding the role of prop-1-ene-1,3-sultone and vinylene carbonate in LiNi<sub>1</sub>/3Mn<sub>1</sub>/3Co<sub>1</sub>/3O<sub>2</sub>/graphite pouch cells: electrochemical, GC-MS and XPS analysis, *J. Electrochem. Soc.* 162 (2015) A2635–A2645 (#JES-15–2503).
- [13] K.J. Nelson, J. Xia, J.R. Dahn, Studies of the effect of varying prop-1-ene-1,3-sultone content in lithium ion pouch cells, *J. Electrochem. Soc.* 161 (2014) A1884–A1889, <http://dx.doi.org/10.1149/2.0791412jes>.
- [14] C.P. Aiken, J. Self, R. Petibon, X. Xia, J.M. Paulsen, J.R. Dahn, A survey of in situ gas evolution during high voltage formation in Li-ion pouch cells, *J. Electrochem. Soc.* 162 (2015) A760–A767, <http://dx.doi.org/10.1149/2.0941504jes>.
- [15] L. Ma, J. Xia, J.R. Dahn, Improving the high voltage cycling of Li[Ni<sub>0.42</sub>Mn<sub>0.42</sub>Co<sub>0.16</sub>]O<sub>2</sub> (NMC442)/graphite pouch cells using electrolyte additives, *J. Electrochem. Soc.* 161 (2014) A2250–A2254, <http://dx.doi.org/10.1149/2.1041414jes>.
- [16] K.J. Nelson, G.L. d' Eon, A.T.B. Wright, L. Ma, J. Xia, J.R. Dahn, Studies of the effect of high voltage on the impedance and cycling performance of Li[Ni<sub>0.4</sub>Mn<sub>0.4</sub>Co<sub>0.2</sub>]O<sub>2</sub>/graphite lithium-ion pouch cells, *J. Electrochem. Soc.* 162 (2015) A1046–A1054, <http://dx.doi.org/10.1149/2.0831506jes>.
- [17] R. Petibon, L. Rotermund, K.J. Nelson, A.S. Gozdz, J. Xia, J.R. Dahn, Study of electrolyte components in Li ion cells using liquid-liquid extraction and gas chromatography coupled with mass spectrometry, *J. Electrochem. Soc.* 161 (2014) A1167–A1172, <http://dx.doi.org/10.1149/2.117406jes>.
- [18] R. Petibon, L.M. Rotermund, J.R. Dahn, Evaluation of phenyl carbonates as electrolyte additives in lithium-ion batteries, *J. Power Sources* 287 (2015) 184–195, <http://dx.doi.org/10.1016/j.jpowsour.2015.04.012>.
- [19] L. Madec, J. Xia, R. Petibon, K.J. Nelson, J.-P. Sun, I.G. Hill, et al., Effect of sulfate electrolyte additives on LiNi<sub>1</sub>/3Mn<sub>1</sub>/3Co<sub>1</sub>/3O<sub>2</sub>/graphite pouch cell lifetime: correlation between XPS surface studies and electrochemical test results, *J. Phys. Chem. C* 118 (2014) 29608–29622, <http://dx.doi.org/10.1021/jp509731y>.
- [20] R. Petibon, J. Harlow, D.B. Le, J.R. Dahn, The use of ethyl acetate and methyl propanoate in combination with vinylene carbonate as ethylene carbonate-free solvent blends for electrolytes in Li-ion batteries, *Electrochim. Acta* 154 (2015) 227–234, <http://dx.doi.org/10.1016/j.electacta.2014.12.084>.
- [21] R. Petibon, C.P. Aiken, N.N. Sinha, J.C. Burns, H. Ye, C.M. VanElzen, et al., Study of electrolyte additives using electrochemical impedance spectroscopy on symmetric cells, *J. Electrochem. Soc.* 160 (2013) A117–A124, <http://dx.doi.org/10.1149/2.005302jes>.
- [22] R. Petibon, N.N. Sinha, J.C. Burns, C.P. Aiken, H. Ye, C.M. VanElzen, et al., Comparative study of electrolyte additives using electrochemical impedance spectroscopy on symmetric cells, *J. Power Sources* 251 (2014) 187–194, <http://dx.doi.org/10.1016/j.jpowsour.2013.11.054>.
- [23] G.-Y. Kim, R. Petibon, J.R. Dahn, Effects of succinonitrile (SN) as an electrolyte additive on the impedance of LiCoO<sub>2</sub>/graphite pouch cells during cycling, *J. Electrochem. Soc.* 161 (2014) A506–A512, <http://dx.doi.org/10.1149/2.014404jes>.
- [24] S. Tanuma, C.J. Powell, D.R. Penn, Calculations of electron inelastic mean free paths. V. Data for 14 organic compounds over the 50–2000 eV range, *Surf. Interface Anal.* 21 (1994) 165–176, <http://dx.doi.org/10.1002/sia.740210302>.
- [25] J.C. Burns, R. Petibon, K.J. Nelson, N.N. Sinha, A. Kassam, B.M. Way, et al., Studies of the effect of varying vinylene carbonate (VC) content in lithium ion cells on cycling performance and cell impedance, *J. Electrochem. Soc.* 160 (2013) A1668–A1674, <http://dx.doi.org/10.1149/2.031310jes>.
- [26] R. Petibon, E.C. Henry, J.C. Burns, N.N. Sinha, J.R. Dahn, Comparative study of vinyl ethylene carbonate (VEC) and vinylene carbonate (VC) in LiCoO<sub>2</sub>/graphite pouch cells using high precision coulometry and electrochemical impedance spectroscopy measurements on symmetric cells, *J. Electrochem. Soc.* 161 (2014) A66–A74, <http://dx.doi.org/10.1149/2.030401jes>.
- [27] L. Madec, R. Petibon, J. Xia, J.-P. Sun, I.G. Hill, J.R. Dahn, Understanding the role of prop-1-ene-1,3-sultone and vinylene carbonate in LiNi<sub>1</sub>/3Mn<sub>1</sub>/3Co<sub>1</sub>/3O<sub>2</sub>/graphite pouch cells: electrochemical, GC-MS and XPS analysis, *J. Electrochem. Soc.* 162 (2015) A2635–A2645, <http://dx.doi.org/10.1149/2.0741512jes>.
- [28] J. Self, D.S. Hall, L. Madec, J.R. Dahn, The role of prop-1-ene-1,3-sultone as an additive in lithium-ion cells, *J. Power Sources* 298 (2015) 369–378, <http://dx.doi.org/10.1016/j.jpowsour.2015.08.060>.
- [29] H. Kim, S. Grugeon, G. Gachot, M. Armand, L. Sannier, S. Laruelle, Ethylene bis-carbonates as telltales of SEI and electrolyte health, role of carbonate type and new additives, *Electrochim. Acta* 136 (2014) 157–165, <http://dx.doi.org/10.1016/j.electacta.2014.05.072>.
- [30] G. Gachot, S. Grugeon, M. Armand, S. Pilard, P. Guenot, J.-M. Tarascon, et al., Deciphering the multi-step degradation mechanisms of carbonate-based electrolyte in Li batteries, *J. Power Sources* 178 (2008) 409–421, <http://dx.doi.org/10.1016/j.jpowsour.2007.11.110>.
- [31] D. Aurbach, M.D. Levi, E. Levi, A. Schechter, Failure and stabilization mechanisms of graphite electrodes, *J. Phys. Chem. B* 101 (1997) 2195–2206, <http://dx.doi.org/10.1021/jp962815t>.
- [32] J.-M. Atebamba, J. Moskon, S. Pejovnik, M. Gaberscek, On the interpretation of measured impedance spectra of insertion cathodes for lithium-ion batteries, *J. Electrochem. Soc.* 157 (2010) A1218–A1228, <http://dx.doi.org/10.1149/1.3489353>.
- [33] K. Xu, A. von Cresce, U. Lee, Differentiating contributions to “ion transfer” barrier from interphasial resistance and Li<sup>+</sup> desolvation at electrolyte/graphite interface, *Langmuir* 26 (2010) 11538–11543, <http://dx.doi.org/10.1021/la1009994>.
- [34] N. Ogihara, S. Kawauchi, C. Okuda, Y. Itou, Y. Takeuchi, Y. Ukyo, Theoretical and experimental analysis of Porous electrodes for lithium-ion batteries by electrochemical impedance spectroscopy using a symmetric cell, *J. Electrochem. Soc.* 159 (2012) A1034–A1039, <http://dx.doi.org/10.1149/2.057207jes>.
- [35] M.B. Pinson, M.Z. Bazant, Theory of SEI formation in rechargeable batteries: capacity fade, accelerated aging and lifetime prediction, *J. Electrochem. Soc.* 160 (2013) A243–A250, <http://dx.doi.org/10.1149/2.044302jes>.
- [36] D. Aurbach, B. Markovsky, I. Weissman, E. Levi, Y. Ein-Eli, On the correlation between surface chemistry and performance of graphite negative electrodes for Li ion batteries, *Electrochim. Acta* 45 (1999) 67–86, [http://dx.doi.org/10.1016/S0013-4686\(99\)00194-2](http://dx.doi.org/10.1016/S0013-4686(99)00194-2).
- [37] J.R. Dahn, Phase diagram of Li<sub>2</sub>C<sub>6</sub>, *Phys. Rev. B* 44 (1991) 9170–9177, <http://dx.doi.org/10.1103/PhysRevB.44.9170>.
- [38] D.P. Abraham, J. Liu, C.H. Chen, Y.E. Hyung, M. Stoll, N. Elsen, et al., Diagnosis of power fade mechanisms in high-power lithium-ion cells, *J. Power Sources* 119–121 (2003) 511–516, [http://dx.doi.org/10.1016/S0378-7753\(03\)00275-1](http://dx.doi.org/10.1016/S0378-7753(03)00275-1).
- [39] D.P. Abraham, R.D. Twisten, M. Balasubramanian, I. Petrov, J. McBreen, K. Amine, Surface changes on LiNi<sub>0.8</sub>Co<sub>0.2</sub>O<sub>2</sub> particles during testing of high-power lithium-ion cells, *Electrochem. Commun.* 4 (2002) 620–625, [http://dx.doi.org/10.1016/S1388-2481\(02\)00388-0](http://dx.doi.org/10.1016/S1388-2481(02)00388-0).
- [40] S. Watanabe, M. Kinoshita, T. Hosokawa, K. Morigaki, K. Nakura, Capacity fade

- of  $\text{LiAl}_y\text{Ni}_{1-x-y}\text{Co}_x\text{O}_2$  cathode for lithium-ion batteries during accelerated calendar and cycle life tests (surface analysis of  $\text{LiAl}_y\text{Ni}_{1-x-y}\text{Co}_x\text{O}_2$  cathode after cycle tests in restricted depth of discharge ranges), *J. Power Sources* 258 (2014) 210–217, <http://dx.doi.org/10.1016/j.jpowsour.2014.02.018>.
- [41] F. Lin, I.M. Markus, D. Nordlund, T.-C. Weng, M.D. Asta, H.L. Xin, et al., Surface reconstruction and chemical evolution of stoichiometric layered cathode materials for lithium-ion batteries, *Nat. Commun.* 5 (2014) 3529, <http://dx.doi.org/10.1038/ncomms4529>.
- [42] J. Self, C.P. Aiken, R. Petibon, J.R. Dahn, Survey of gas expansion in Li-ion NMC pouch cells, *J. Electrochem. Soc.* 162 (2015) A796–A802, <http://dx.doi.org/10.1149/2.0081506jes>.
- [43] J.C. Burns, A. Kassam, N.N. Sinha, L.E. Downie, L. Solnickova, B.M. Way, et al., Predicting and extending the lifetime of Li-ion batteries, *J. Electrochem. Soc.* 160 (2013) A1451–A1456, <http://dx.doi.org/10.1149/2.060309jes>.
- [44] A. Jarry, S. Gottis, Y.-S. Yu, J. Roque-Rosell, C. Kim, J. Cabana, et al., The formation mechanism of fluorescent metal complexes at the  $\text{Li}_x\text{Ni}_{0.5}\text{Mn}_{1.5}\text{O}_{4-\delta}$ /carbonate ester electrolyte interface, *J. Am. Chem. Soc.* 137 (2015) 3533–3539, <http://dx.doi.org/10.1021/ja5116698>.
- [45] S.R. Li, C.H. Chen, X. Xia, J.R. Dahn, The impact of electrolyte oxidation products in  $\text{LiNi}_{0.5}\text{Mn}_{1.5}\text{O}_4/\text{Li}_4\text{Ti}_5\text{O}_{12}$  cells, *J. Electrochem. Soc.* 160 (2013) A1524–A1528, <http://dx.doi.org/10.1149/2.051309jes>.